Journal of Mechanical Engineering Research and Developments
ISSN: 1024-1752
CODEN: JERDFO
Vol. 44, No. 1, pp. 28-40
Published Year 2021

Preparation And Characterization Of Hydroxyapatite Coating On F75 Alloy Implant Using Pulse Laser Deposition

Nawal Mohammed Dawood, Ahmed Saleh AlGraiti, Zainab Mohammed Lafta

Dept. of Metallurgical Engineering ,College of Materials Engineering, University of Babylon, Babylon-Iraq.

*Corresponding Author Email: mat.newal.mohammed@uobabylon.edu.iq, ahmed.agc040@gmail.com, alihhk64@ gmail.com

ABSTRACT: CoCrMo alloys have involved substantial considerations as orthopedic implants due to their extraordinary biocompatibility and reliable mechanical behavior and properties. Though, comparable to additional bioinert metallic implants, CoCrMo alloys displays reduced bioactivity. So, it does not improve direct chemical bonding with host bone tissue that can lead to the implant failure. Consequently, the request of bioactive coatings on the metallic implants is essential in order to attain adequate bioactivity. Further, the request of coatings significantly reduces the rate of corrosion of metallic implant and so the release of toxic metallic ions into the nearby tissue. Hydroxyapatite (HA) coatings on the metallic implants have showed decent fixation to host bone and enhanced bone ingrroth into the implant. HA is the generally manufactured from both Calcium (Ca) and Phosphate (P) to produce (Ca10(PO4)6(OH)2) that used as a base material for covering mineral embeds because of its incredible biocompatibility and comparable the synthesis and structure to sclerous tissues of the human body. HA coatings on CoCrMo (F75) alloy substrates have been produced by Pulsed laser deposition (PLD) techniques. HA used in this search pressed at pressure (150MPa) with particle size (2.75 μm) and used as a target in the coating by (PLD) techniques. Surface characterization studies of the coatings such as XRD, SEM, AFM, and EDS to detect the amount of (Ca) and (P) in the coating layer were carried out. Then test the micro-hardness, surface roughness for HA coating. Corrosion behavior for uncoated and coated samples with a various number of pulses in Hank's solution by using potential static polarization tests was achieved also, in this test we obtained a greatly improved in corrosion resistance of the samples B3 after coating by 88.91%.

KEYWORDS: Co-Cr-Mo Alloy, biocompatibility., Hydroxyapatite (HA), Corrosion Rate, Pulsed laser deposition (PLD)

INTRODUCTION

The Co-based alloys, such as CoCrMo and CoCr have been spread used as the main materials for orthopedic application for the total hip, total knee, and total joint replacements due to its outstanding properties regarding its resistance to wear [1-4]. However, the CoCrMo, as considered as an ion tolerant material, has showed difficulties to bond or connect directly to the hard and stiff tissues because of fibrous tissue encapsulations [5,6]. The metallic implants are coated with a bioactive layer of the calcium phosphate (CaP), octacalcium phosphate (OCP), and hydroxyapatite (HA) [7-12] in order to improve the ability of bone bending. Other alloys, such as cobalt and titanium are coated by a HA by using a physical treatment, such as the thermal spray method, for enhancing the biocompatibility [13–15]. Though, the structure of the HA coating may be destroyed by this treatment because of the harmful effect of the strong heat on the substrate [16]. In addition, most of the modified physical treatment accomplished on the implants are the line-of-sight processes that, sometimes, is not suitable for the prosthetic of the complex shapes [16]. Some researchers have used an alternative method instead of the physical treatment. They mentioned the deposition of the calcium composite as a coating on the Co-based alloys by using method of investment casting [17].

The calcium composite have used for coating the surface of the CoCrMo. These coating are applied in different layers, such as $Ca_3(PO_4)_2$ and HA to the surface by casting process at high temperature. However, the coating layer decomposition may be result during the casting process at high temperature [17]. The Co-Cr based alloys performance has driven the investigators for studying their corrosion behavior, mechanical properties, and the tolerance degree by tissues under simulated working physiological conditions [18-21]. In their research, Ameer et al. [22] explained the corrosion behavior of Co-Cr and Ni-Cr base alloys by using the electrochemical impedance and potentiodynamic polarization techniques. Authors concluded that Co-Cr-Mo alloys are the alloys

that showed the higher resistance of the corrosion compared to Ni-Cr-Mo alloys. Mareci et al. [23] studied behavior of corrosion of Co-Cr (Vitallium 2000) alloys and Ag–Pd alloys subjected to artificial saliva by using the electrochemical impedance spectroscopy and potentiodynamic polarization techniques.

Their results showed that the Vitallium2000 presented an outstanding resistance to the corrosion and this alloy can be used as substitution alloy to Ag–Pd alloys for fabrication several elements of the fixed prosthetic applications. Effect of the porcelain-fused-to-metal (PFM) firing process on the behavior of the corrosion of Co–Cr alloys used for dental applications was evaluated by Qiu et al. [24]. Their study was accomplished by electrochemical impedance spectroscopy tests. They showed that, the corrosion resistance, after the firing of PFM, for the low Mo-containing Co–Cr alloy decreased with the decreasing in the oxygen level and Cr in the surface of the oxides. Hodgson et al [25] studied the CoCrMo alloy electrochemical properties when subjected to the body conditions and the transpassive and passive states of the relevant mechanism. Potentiostatic polarization, rotating disc electrode, cyclic voltammetry, potentiodynamic, and electrochemical impedance spectroscopy, as some of the electrochemical techniques, were used in their work. They found that the passive film on the CoCrMo varied in the thickness and composition with both time and potential. In addition, the main passive behavior was because of highly enriched (≈90% Cr oxides) oxide film formation on the surface of the alloy. The transpassive and passive behaviors is then dominated by the presence of the Cr element.

In recent years, an increasing interesting in the HA and OCP coating preparation methods has been noticed especially for the biomaterial regarding the wet chemical methods [26-31]. Good information and review can be seen in [1] about the coating formation of the calcium phosphate. The chemical treatment, among the wet chemical methods, in alkaline solution presented a good method that can be used for enhancing the HA coating growth on the titanium implants. An intermediate layer of $CaTiO_3$ or Na_2TiO_3 , as a result of the treatment, has been formed as a result of the treatment. An ion exchange of H^+ and Na^+ induced an environment of high value of pH around the surface when immersion in SBF.

This led for precipitation of insoluble species of calcium phosphate. Kim and Wei et al. applied this type of the chemical treatment on tantalum and titanium alloys and the it was smoothly succeeded [26–28], where they reported that HA coatings with about 10 μm thickness formed on Ti and Ta by immersion in SBF for up to 4 weeks. Recently, Xie and Luan modified the method [26–30] by electrochemical etching and obtained an HA layer on Ti alloys in very short immersion time [31]. Thus, the purpose of this work is to investigate the corrosion behavior of F75 alloy in Hank's solution for their potential application as biomaterial.

MATERIALS AND METHODS

Sample Preparation

The material powders used to prepare (F75) Co-Cr-Mo alloys in this work are demonstrated in Table 1.The average size of particle was calculated using Better size 2000 laser particles size analyzer, Handheld (XRF) analyzer type (DS-2000)USA, is used to determine the purity of powders. Electrical rolling mixer type (STGQM-1/5-2) used in elemental powders mixing process for (5hr). the applied stress was 800MPa on the metallic powders to get green compacted samples by using the electric hydraulic press in a cylindrical die in one direction to produce cylindrical samples with a diameter 10mm.

Vacuum tube furnace type MTI (GSL1600X)was used to sinter samples from room temperature to 500 ℃ and soaking 2 hr then heating to 950 ℃ and then soaking for 5hr and then slow cooling to room temperature. All samples after sintering process were grinded utilizing (180, 220, 320, 600, 800, 1000,1200,1500,2000 and 2500) grit SiC sandpaper, then they were polished using a diamond past of 15 μm for obtaining a bright mirror finishing that ready for the next step. Etching was made at room temperature (60ml HCl, 15ml HNO_3. 15ml acidic acid & 15ml water) [32]. After the process of etching, samples were washed in water and then dried. The sintered samples porosity is calculated as per ASTM B-328 [33].

Table 1. Purity % and Average Size of Material's Particles

Material (powder)	**Purity %**	**Average Size of Particle (µm)**	**Chemical Composition% F75**
Cobalt	99.61	55.56	Balance
Chrome	99.86	40.52	28%
Molybdenum	99.28	20.33	6%
Manganese	99.39	52.31	1%
Nickel	99.44	43.26	0.5%
Silicon	99.11	51.47	1%
Iron	99.77	59.34	0.75%
Carbon	99.44	37.44	0.35%

Pulsed Laser Deposition PLD

Powder and target preparations

A 20 g of HA powder was collected and processing beginning with manual grinding utilizing mortar for getting the semi-finished powder. The next step is sieving the powder utilizing 200 meshes sieve number. Subsequently, the powder has been crushed and milled for obtaining a nano-sized powder utilizing a planetary ball milling. The milling was done for 24 h at 350 rpm.

The particle size of the powder obtained from milling process was measured using particle size analyzer Bettersize 2000 laser particle size analyzer. The powder was (0.668-12.99) µm. Then, the powder was mixed with 3mL of Poly Vinyl Alcohol (PVC) as a binding material. Then, the mixture was mold in (Ø20 mm) and pressed at pressure 150 MPa, after that, the target was dried using the dry box at 150 ℃ for 4h dehumidify and PVC releasing (Fig. 1).

PLD Coating Process

In this step, targets have been placed on a rotator holder (Fig. 2) [**34**] and ablated using excimer lasers with pulses of Ar F (λ=1064nm) and applied energy of (600) m J. The area of ablate was about 20mm^2 and the pulses number was within (1500-6000). Thin layers have been deposited on F75 alloy substrate heated at a temperature 300 ^{o}C. The distance of target substrate was 3 cm and the PLD chamber's inside pressure was 1.5x 10^{-5} torr. The samples coding shown in the Table 2 While Table 3 summarize the HA Deposition Parameter.

Figure 1. One of Targets after Pressing Process

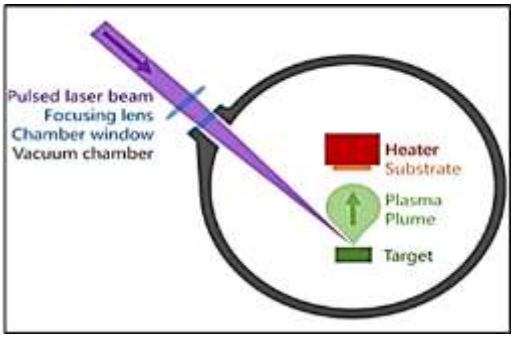

Figure 2. Schematic of the PLD Process,[34].

Table 2: Samples code

Parameter	Available ranges	Selected value
Power	1-1000 m J	1000 mJ
Frequency	1-6 Hz	6 Hz
Pulses	1-15000	4000-6000-8000
Laser wave length	1064 nm	1064nm
Pulse duration	10 n sec	10 nsec
Vacuum pressure	10-5 mbar	10-5 mbar

Table 3. HA Deposition Parameter

Samples code	A	B1	B2	B3
Number of pulses	uncoated	4000	6000	8000

Annealing Process

The deposited films were post-annealing at temperature 450 ^{o}C for 1 h in vacuum process ((10^{-4}) tor at heating rate 5 ^{o}C/min.

Characterizations technique

In the current work, the following tests were performed to evaluate the performance of HA coating layer on F75 substrate.

XRD Analyzer

Sample with dimensions (d=10mm , t=5 mm) was used for X-ray diffraction characteristics using XRD type Mini flex2. X-ray generator with CuKα radiation at 30.0 mA and 40.0 kV is used, the instrument was held at scan speed (2^{o}/min), with step 0.02^{o}/sec.

SEM and EDS Analyzer

In present work scanning electron microscopy model (TESCAN S8000, USA) with the energy-dispersive spectroscopy (EDS) is used to characterize the morphology and microstructure of the coating surface in terms of uniformity.

AFM Analyzer

Atomic force microscopy (AFM, contact mode, spm AA3000 Angstrom advanced Inc., USA) was employed for observing the morphology (depth morphology of film and roughness) .

Thickness Test

The measuring device of thickness was utilized for measuring the HA films thickness on F75 substrates.

Hardness Test

Vickers Hardness (TH-717 Digital Micro Vickers Hardness Tester) was utilized to measure the hardness of HA films, at load (300g) and time of holding equals to 15 sec.

Electrochemical Test

The corrosive behavior of F75 alloy studied in Hank's solution. The chemical analysis for Hank's solution is illustrated in Table 4 [**35**]. and pH of it at 37C° was 7.4.

Table 4. Chemical Composition of Hanks Solutions [35]

No.	Constituent	(g/L)
1	NaCl	8
2	$CaCl_2$	0.14
3	KCl	0.4
4	$NaHCO_3$	0.35
5	Glucose	1
6	$MgCl_2.6H_2O$	0.1
7	$Na_2HPO_4.2H_2O$	0.06
8	KH_2PO_4	0.06
9	$MgSO_4.7H_2O$	0.06

The test was performed by gradual increasing in the potential by a scanning ratio equals to 0.4 mV/s, that starting from 450 mV lower than the potential of open circuit and the scanning was kept on up to 450 mV higher than the potential of open circuit. Measurement of corrosion rate was obtained via applying the equation (1)[36].

$$\text{Corrosion rate (mpy)} = 0.13 i_{corr}.(E.W.)/A.\rho \quad (1)$$

Where: E.W. indicates the equivalent weight (g/eq), A is the area measured in (cm^2), ρ denotes to the density (g/cm^3), 0.13 is the metric and time conversion factor, icorr. Denotes to the density of current (μA /cm^2).
The percentage of improvement for coated samples can be calculated utilizing the equation (2) [36]

$$\text{Percentage of improvement} = (CR0 \_ CR / CR0) * 100 \quad (2)$$

Where: CR° represents the corrosion rate of uncoated sample. CR =the corrosion rate of coated sample (with HA coated).

RESULTS AND DISSCUSIONS

Co-Cr-Mo (F75) characterization

Fig. 3 illustrated the XRD patterns for A sample after sintering at 950 ℃ for 5 hours under controlled atmosphere. It can be observed that all Co, Cr and Mo transformed to (CoCrMo), (CoCr) and (Co_2Mo_3) phases. This means that the sintering process period (5 hr) was enough to complete the phase transformation process, where transformation of the phase represents a diffusion process and it requires a high temperature to take place. The absence of free element is necessary in the alloys which used as biomaterials due to it toxicity effect into body. The peaks match with the standard chart of the X-ray diffraction for each phase. The SEM images are highly sensitive to the chemical composition; therefore, the sintered samples microstructure exhibited a multiphase structure where the two phases (CoCr and Co_2Mo_3) are embedded in uniformly matrix (CoCrMo – F.C.C), thus confirming the XRD results. Etched alloys SEM images exhibited the grain boundaries and pores with different sizes (Fig.4). The result of EDS analysis for F75 sample is shown in Fig. 5. Provided the presence of Co and Cr as base alloy with Mn, Ni, Si as additional element, Also the EDS show no evidence of Mo elements other than Co and Cr as base alloy. Clearly, the EDS analysis results were fairly close to the addition percentage, as the values obtained from EDS analysis did not cover the entire area but only the spotted region where the electron

stroke. Furthermore, the EDS results aide in verifying the purity of the initial elemental powders as well as the prevention of contamination during casting and the production of alloys [37].

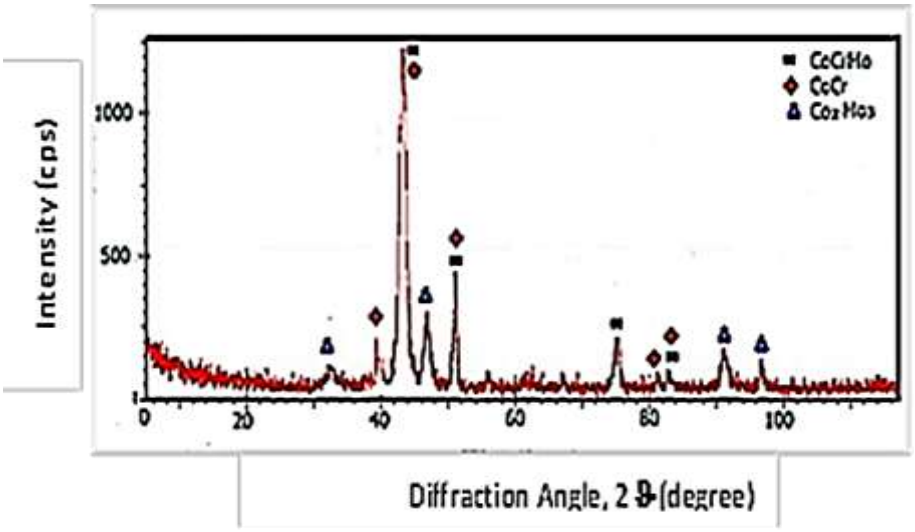

Figure 3. XRD Pattern of Co-Cr-Mo alloy After Sintering

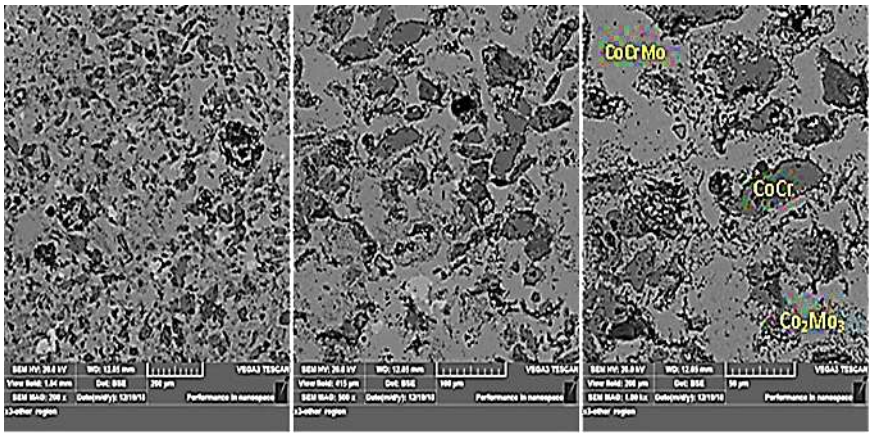

Figure 4. SEM images for etched A alloy with different magnification

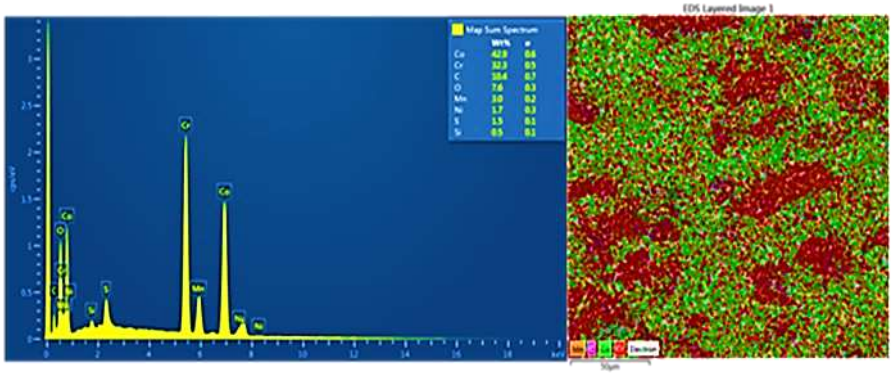

Figure 5. EDS Analysis for sample A

Coating characterization

XRD results

The XRD results of HA powder in the range 10° -50° diffracted angle are shown in the Fig. 6. The pattern refers to the existence peaks of HA phase $Ca_{10}(PO_4)_6(OH)_2$. Fig.7. shows the XRD pattern of the HA thin films after

annealing on F75 alloy produced by PLD technique. The XRD results implies that only HA phase can be detected on the coating , which indicates that Hydroxyapatite coating was succeeded on F75 alloy by PLD technique. There are several obvious diffraction peaks observed at 43°,32°,33° and 22° representing the peaks of HA phase. Peaks of CoCrMo , CoCr, Co_2Mo_3 comes from the substrate because the PLD coating on F75 alloy is so thin that the X-ray can penetrate it.

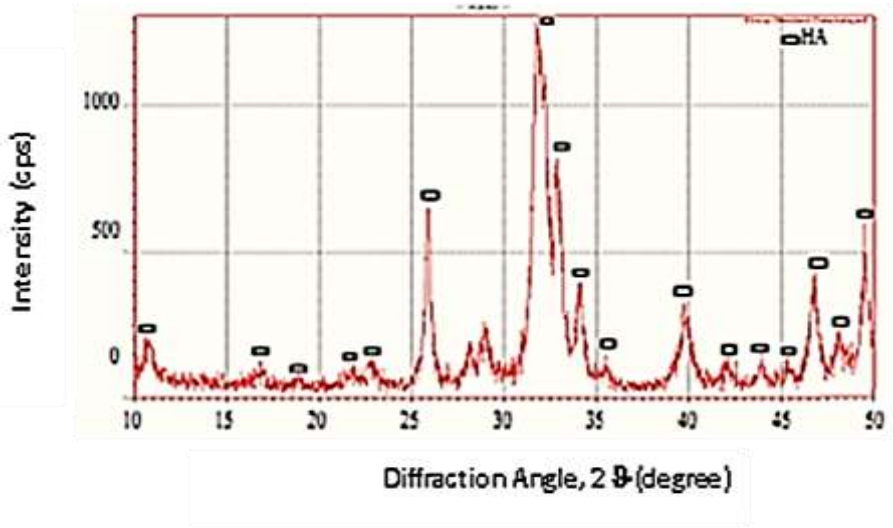

Figure 6. XRD Patterns of HA powder

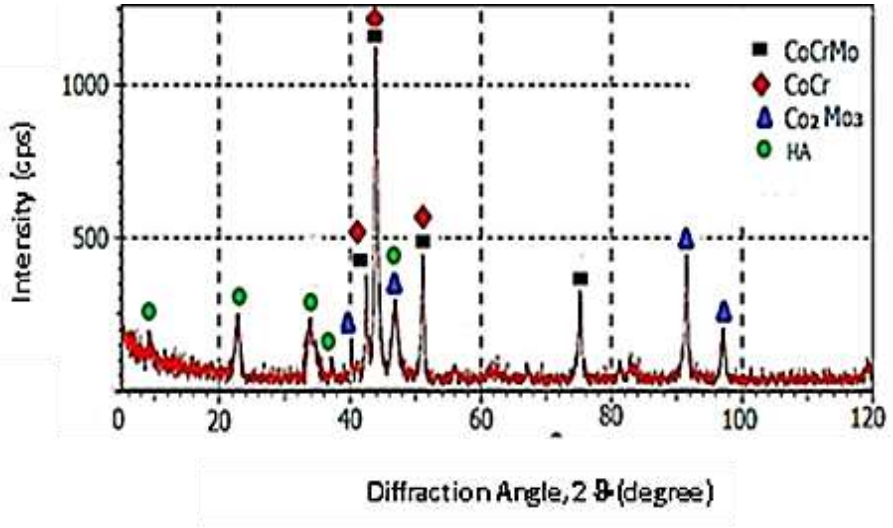

Figure 7. XRD analysis of HA film

SEM and EDS Results

Fig. 8. shows SEM micrographs of 200MPa HA samples deposited at different pulses and at 300˚C substrate temperature. It was obviously seen that increasing the pulses from 4000 to 8000 results in improvement of the HA films. The HA particles were deposited to create clusters on the base material that looks like a heavy and aggregated composition. Furthermore, more pulses will be beneficial in improving the film growing, density and microstructure. The percentages of (Ca), (O) and (P) of HA films and for (Ti) for the samples (B1, B2, B3) are shown in Fig. 9 respectively. As the number of pulses increase the ratio of (Ca) and (P) increases in the coating layer. This is expected due to the surface and the corresponding EDS elemental spectrum of the specimens that were coated with HA at various pulses, some particles and agglomerates had been noticed. On the other hand, the EDS analysis shows the existence of P, Ca, and O with the absence of alloying elements of substrate. Peaks that corresponding to P and Ca exhibited an intensity increasing with increasing the number of pulses from 4000 to 8000 and the alloying elements cannot be distinguished on the HA coated samples. This implies that the ceramic

layer thickness increased with increasing amount of HA precipitation as the pulse increases. These results are in agreement with those given by El-Sayed et al [38].

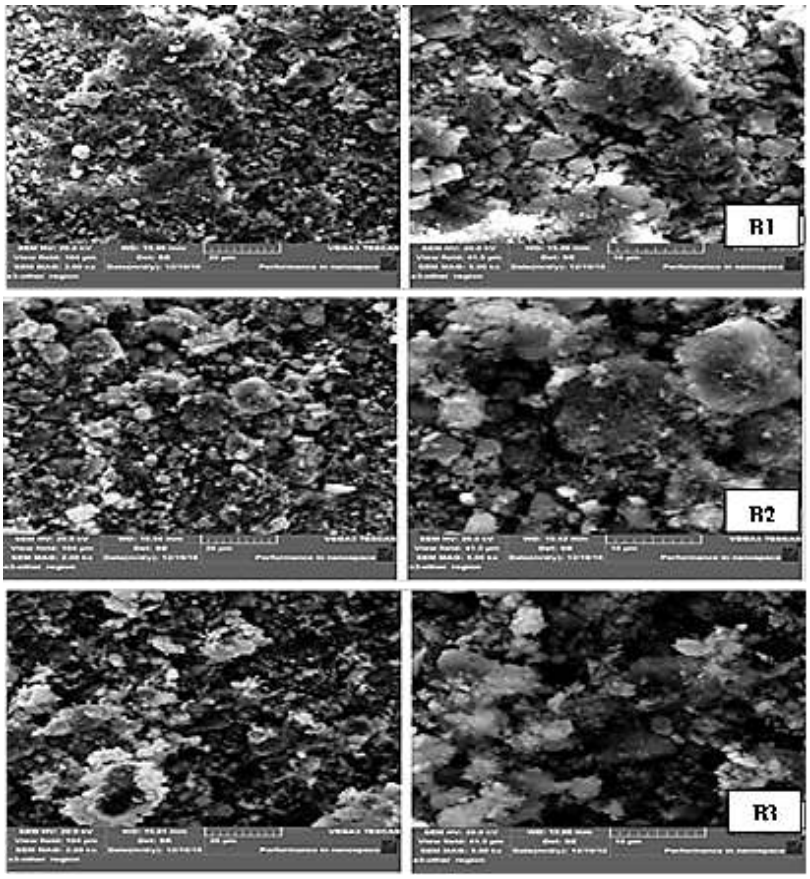

Figure 8. SEM micrograph of the samples B1, B2, and B

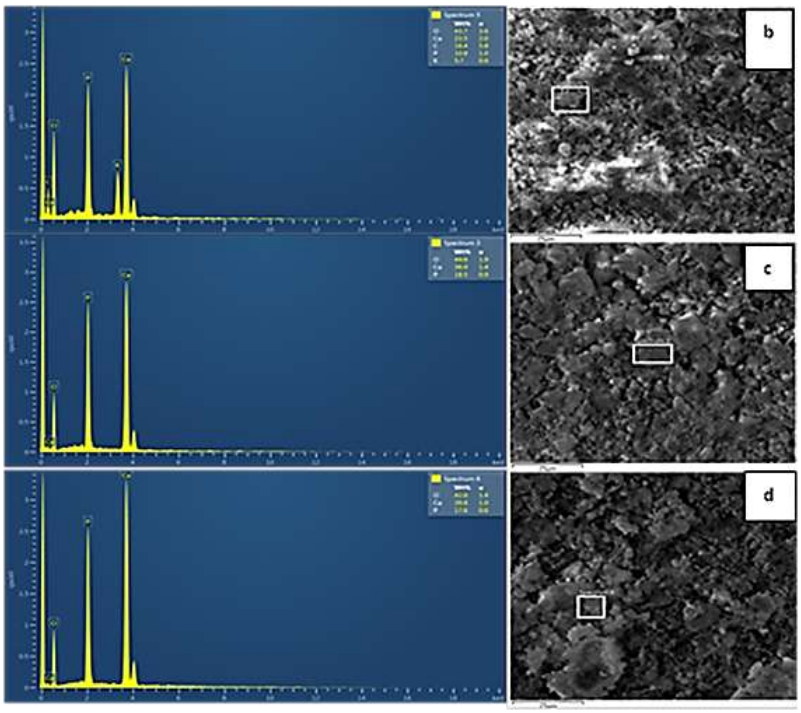

Figure 9. EDS Analysis of the samples b) B1, c) B2, and d) B3

AFM Results

Fig. 10(a- c) exhibits the images obtained from AFM test of the coated HA films on the samples with 4000, 6000 and 8000 pulses after annealing, respectively. The topographies reveal that increasing the pulses number led to increase the roughness of the sample surface. Therefore, the distances located between the valleys and peaks of the sample deposited at 8000 pulses (Fig. 10c) are relatively large. The samples' surface roughness involving Ra (average height on top of center line) and Rz is listed in Table 5. Former studies indicated that rough and porous implant surface could mainly increase the bone bioactivity and its ability of bonding [39, 40]. It is well known that a rough and porous structure improves the supplying of blood and oxygen along with the ingrowth of the bone and anchoring at the interface [41]. Consequently, sample that was coded B3 in Table 5 with the Ra of 29.84 nm and Rz of 192.21 nm is the best surface roughness.

Thickness Results

For B1 sample, the thickness is 1.8 μm. The thickness is increased to 2.4 μm for B2 sample and then, the thickness is reach to its high value 3.6 μm for B3 sample. Anyhow, with increasing the number of laser pulses, the deposition rate is increased and the thickness is increased also.

Hardness Results

Hardness of uncoated samples F 75(184 HV) are improved after coating it with HA. Furthermore increasing of pulses from 4000 to 6000 to 8000 could improve the hardness from (254 HV) to (263 HV) to (279 HV). These results are agreement with P. Rajesh et.al, [42], Such improvement is due to the improvement in depth morphology, distribution and increasing in HA thickness which can be clearly observed as SEM results as in Fig. 8 and as AFM results in Fig 10. Most likely the pulse increasing could implant more HA particles on the substrate surfaces.

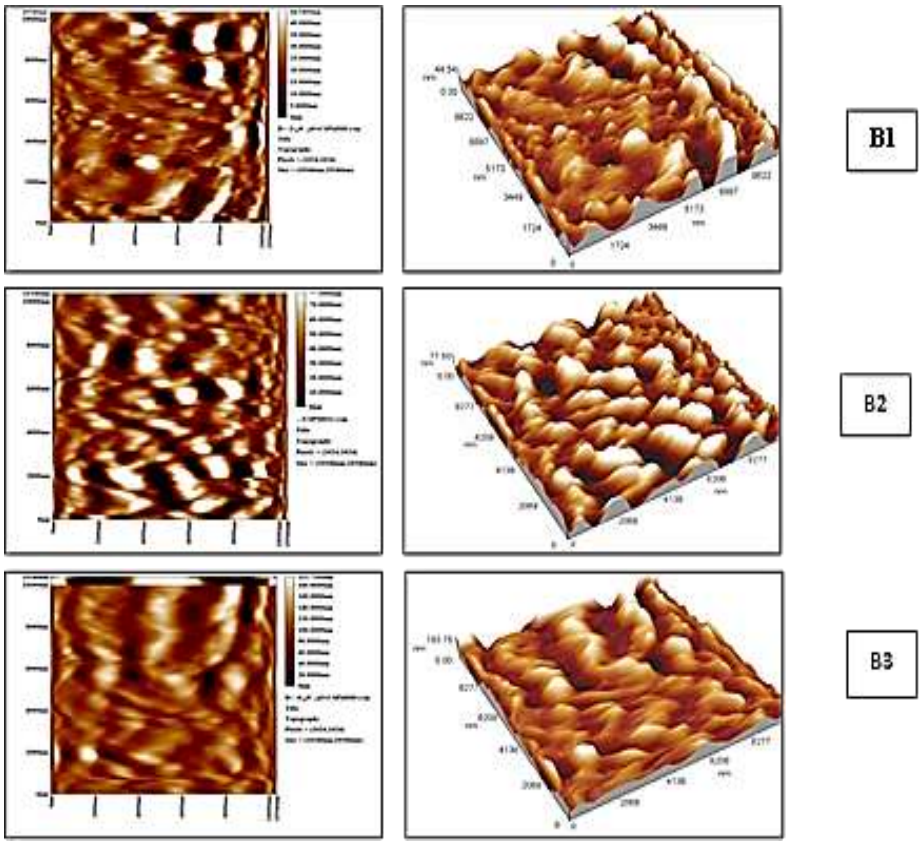

Figure 10. AFM pattern of samples at : B1, B2, and B3 after the annealing treatment

Table 5. The Effect of Laser Pulses on Surface Roughness of HA coating.

Sample code	Surface Roughness	
	Ra(mm)	Rz (mm)
B1	7.87	44.42
B2	16.81	77.52
B3	29.84	192.21

Corrosion Results

Potentiostatic Polarization

The potentiostatic polarization test was achieved utilizing the Potentiostatic polarization test in Hank's solution for uncoated (F75) and HA coated samples at temperature equals to 37 °C, Polarization curves are shown in Fig 11. Corrosion parameters (corrosion potential, corrosion current, and corrosion rate), extracted from these curves, are listed in Table 6. The corrosion potential of all coated samples shows a significant shift to a positive direction and have more noble potential compared to uncoated sample. Further, it is clear that (B1, B2,and B3) samples have current densities and corrosion rate much lower than current densities and corrosion rate of uncoated sample, which indicate that HA coating acts as a barrier against attack of aggressive ions, affectively improve the corrosion resistance of F75 alloy implant, [43],[44]. Corrosion ratio for the implant inside lives' bodies can be reduced by coating the sampling with HA, due to the reduction in iron releasing from the metal surface. Where the HA has a favorite characteristics which lead to applied it widely in different implants protection. One of the implantation process requirements for prostheses, there should be a contact between the tissue around the bones and the metal prosthesis. Where the availability of HA in metal coating for the implant will lead to produce the bonding rapidly between the tissue around the bones and the metal prosthesis. Many reasons lead to apply the HA in coating the implant because HA is a biocompatible material so the implants have both strength and biocompatible at the same time which lead to induce the ingrowths of bone and tissue surrounding it as well as the chemical reactions that produce bonding. Also, the availability of HA in implants metal coating will increase the resistance of the metal against corrosion in condition of soaking the metals in biotic solutions by strengthen the chemical bonds and decrease the metal iron releasing [45],[46].

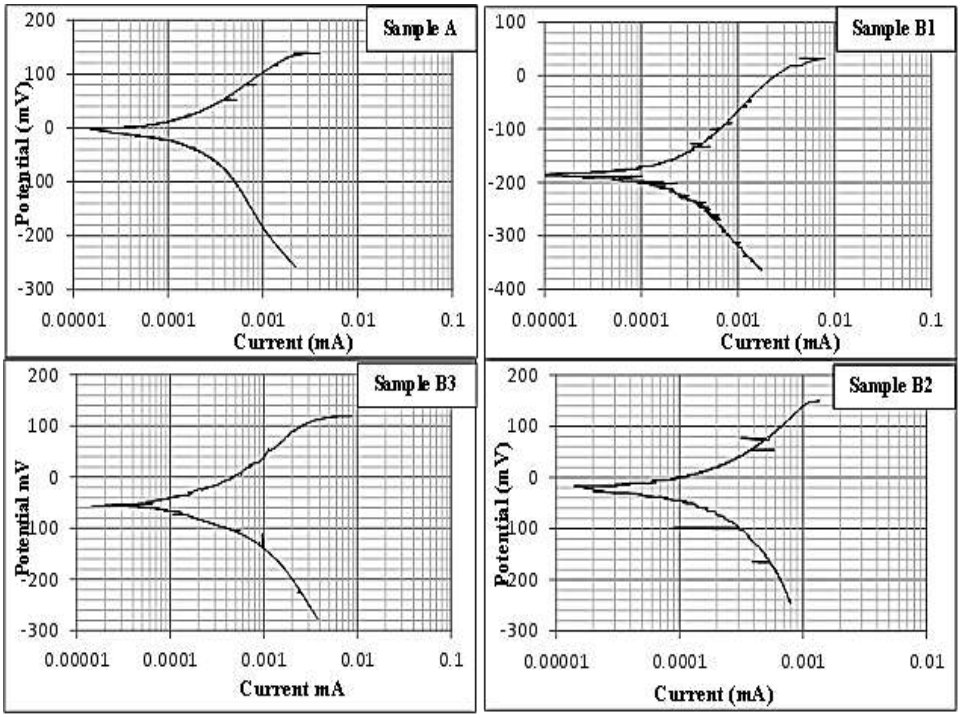

Figure 11. Potentiostatic Polarization for A, B1,B2, and B3 samples in Hank′s Solution at 37 °C

Table 4. Illustrate the Corrosion Potential (Ecorr.), Corrosion Current (icorr.), Corrosion Rate (CR) and Improvement Percentage of coated Samples in Hank's solution.

Sample code	Icorr. nA/cm^2	Ecorr. mV	Corrosion Rate (mpy)*10^{-2}	Improvement Percentage%
A	208.15	-36.5	7.992	-
B1	99.50	-185.4	3.824	52.15
B2	50.16	55.8	1.925	75.91
B3	23.07	23.9	0.886	88.91

CONCLUSIONS

Based on the obtained results, the following conclusions are made:

1. The films hardness increased form (184 HV) for uncoated sample to (279HV) for B3 coated sample
2. The thickness of HA film increased with increasing the number of pulses from (1.8 μm) for B1sample to (3.6 μm) for B3 sample.
3. Increasing number of pulses is more beneficial in films growing and distribution.
4. In Hank's solution however, the most improvement percentage in corrosion rate was (88.91) which achieved in case of using 8000 pulse.
5. Another interesting increasing in biocompatibility was achieved during the work for the coated sample compare to the uncoated F75 alloy.

RECOMANDATIONS

1. Change pulse laser deposition parameters and investigate the effect of these changes on the coating thickness and corrosion rate.
2. Study the effect of heat treatments before and after deposition process.
3. Study of the effect of adding titania to hydroxyapeptite on the corrosive behavior of the alloy

REFERENCES

[1] J.R. Davis, "ASTM International, Medical Applications: Metallic Materials, Handbook of Materials for Medical Devices", American Society for Metals, Pp. 21, 2003.

[2] J. Black, "Biological Performance of Materials: Fundamentals of Biocompatibility", 3rd ed. New York: Marcel Dekker; Pp. 245, 1999.

[3] J.A. Savio III, L.M. Overcamp, J. Black, "Size and shape of biomaterial wear debris", Clin. Mater., Vol. 15, Pp. 101, 1994.

[4] K.A. Martinelli, D.T. Lemaitre, T.J. Lee, "Orthopedic Industry: Update and Company Models", 1st ed. New York: Merrill Lynch, Pp. 11, 2001.

[5] G.M. Keegan, I.D. Learmonth, C.P.Case, "Orthopaedic metals and their potential toxicity in the arthroplasty patient: a review of current knowledge and future strategies", J. Bone Joint Surg Br., Vol. 89B, Pp. 567, 2007.

[6] Annual Report. "The Swedish National Hip Arthroplasty Register August", 2007. http://www.jru.orthop.gu.se/ 2006 (date last accessed 3 December 2008).

[7] M.J. Cross, E.N. Parish, "A comparison of bilateral uncemented total knee arthroplasty: simultaneous or staged?", J Bone Joint Surg Br., Vol. 87B, Pp. 1073, 2005.

[8] S. Toksvig-Larsen, P. Jorn, L. Ryd, A. Lindstrand, "Hydroxyapatite-enhanced tibial prosthetic fixation", Clin Orthop Relat Res., Vol. 370, Pp. 192, 2000.

[9] P. Dixon, E.N. Parish, B. Chan, J. Chitnavis, M.J. Cross, "Hydroxyapatite-coated, cementless total knee replacement in patients aged 75 years and over", J. Bone Joint Surg Br., Vol. 86B, Pp. 200, 2004.

[10] X. Liu, P.K. Chub, and C. Ding, "High-temperature microstructural characteristics of a novel biomedical

titanium alloy", Mater. Sci. Eng. R., Vol. 47, Pp. 49, 2004.

[11] B. León, Betty, J.A. Jansen, "Thin Calcium Phosphate Coatings for Medical Implants", New York: Springer; 2009.

[12] J.M. Toth, M. Wang, B.T. Esters, J.L. Scifert, H.B. Seim, and A.S. Turner, "Polyetheretherketone as a biomaterial for spinal applications", Biomaterials, Vol. 27, Pp. 324, 2006.

[13] C.Y. Yang, B.C. Wang, W.J. Chang, E. Chang, J.D. Wu, "Mechanical and histological evaluations of cobalt–chromium alloy and hydroxyapatite plasma-sprayed coatings in bone", J. Mater. Sci. Mater. Med., Vol. 8, Pp. 167, 1996.

[14] K.A. Khor, C.S. Yip, and P. Cheang, "Ti–6Al–4V/hydroxyapatite composite coatings prepared by thermal spray techniques", J. Ther. Spray Tech., Vol. 6, Pp. 109, 1997.

[15] K.A. Khor, Y.W. Gu, C.H. Quek, P. Cheang, "Plasma spraying of functionally graded hydroxyapatite/Ti–6Al–4V coatings", Surf Coat Technol, Vol. 168, Pp. 195, 2003.

[16] Y.Z. Yang, J.L. Ong, J.M. Tian, "Deposition of highly adhesive ZrO2 coating on Ti and CoCrMo implant materials using plasma spraying", Biomaterials, Vol. 24, Pp. 619, 2003.

[17] J.C. Escobedo, J.C Ortiz, J.M. Almanza, D.A.Cortés, "Hydroxyapatite coating on a cobalt base alloy by investment casting", Scrip Mater, Vol. 54, Pp. 1611, 2006.

[18] E.N. Codaro, P. Melnikov, I. Ramires and A.C. Guastaldi, Russian J. Electrochem., Vol. 36, Pp. 1117, 2000.

[19] R.A. Silva, M.A. Barbosa, R. Vilar, O. Conde, M.D. Belo and I. Sutherland, J. Mater. Sci.: Mater. in Med., Vol. 5, Pp. 353, 1994.

[20] F. Ozcelik, J. Gulen, A. Akdogan and S. Piskin, Prakt. Metallogr., Vol. 36, Pp. 385, 1999.

[21] L.C. Lucas, R.A. Buchanan, J.E. Lemons and C.D. Griffin, J. Biomed. Mater. Res., Vol. 16, Pp. 799, 1982.

[22] M.A. Ameer, E. Khamis and M. Al-Motlaq, Corr. Sci., Vol. 46, No. 11, Pp. 2825, 2004.

[23] D. Mareci, D. Sutiman, A. Cailean and G. Bolat, Bull. Mater. Sci., Vol. 33, No. 4, Pp. 491, 2010.

[24] J. Qiu, W. Yu and F. Zhang, J. Mater. Sci., Vol. 46, Pp. 1359, 2011.

[25] A.W.E. Hodgson, S. Kurz, S. Virtanen, V. Fervel, C.OA. Olsson and S. Mischler, Electrochim. Acta, Vol. 49, Pp. 2167, 2004.

[26] H.M. Kim, F. Miyaji, T. Kokubo, "Preparation of bioactive Ti and its alloys via simple chemical surface treatment", J. Biomed Mater Res., Vol. 32, Pp. 409, 1996.

[27] H.M. Kim, F. Miyaji, T. Kokubo, "Graded surface structure of bioactive titanium prepared by chemical treatment", J. Biomed Mater Res., Vol. 45, Pp. 100, 1999.

[28] M. Wei, H.M. Kim, T. Kokubo, JH. Evans, "Optimising the bioactivity of alkaline-treated titanium alloy", Mater. Sci. Eng., C., Vol. 20, Pp. 125, 2002.

[29] H.B. Wen, Q. Liu, J.R. De Wijn, K. De Groot, and F.Z. Cui, "Preparation of bioactive microporous titanium surface by a new two-step chemical treatment", J. Mater Sci. Mater. Med., Vol. 9, Pp. 121, 1998.

[30] A. Costantini, G. Luciani, F. Branda, L. Ambrosio, G. Mattogno, L. Pandolfi, "Hydroxyapatite coating of titanium by biomimetic method", J. Mater Sci. Mater Med., Vol. 13, Pp. 891, 2002.

[31] J. Xie, B.L. Luan, "Formation of hydroxyapatite coating using novel chemo-biomimetic method", J. Mater. Sci. Mater. Med., Vol. 19, Pp. 3211, 2008.

[32] T. Odahara, H. Matsumoto and A. Chiba, "Mechanical Properties of Biomedical Co-33Cr-5Mo-0.3N Alloy at Elevated Temperatures", Institute for Materials Research, Tohoku University, Sendai 980-8577, Japan 2008

[33] ASTM B-328, "Standard Test Method for Density, Oil Content, and Interconnected Porosity of Sintered MetalStructural Part and Oil – Impregnated Bearing", ASTM international, 2003.

[34] https://en.wikipedia.org/wiki/Pulsed_laser_deposition#/media/File:Diagram_of_pulsed_laser_deposition.png

[35] A.W. Rajih, N.M. Dawood, F.S. Rasheed, "Corrosion protection of 316L stainless steel by HA coating via pulsed laser deposition technique", J. of Eng. and App. Sci., Vol. 13, No. 24, Pp.10221– 10231, 2018.

[36] N.M. Dawood, "Erosion-Corrosion Behavior of Al-20%Ni-Al2O3 Metal Matrix Composites by Stir Casting", Materials Science Forum, Vol. 1002, Pp. 161-174, 2020.

[37] N.M. Dawood, A.K.A. Ali and A.A. Atiyah, "Fabrication of Porous NiTi Shape Memory Alloy Objects by Powder Metallurgy for Biomedical Applications", IOP Conf. Series: Materials Science and Engineering, Vol. 518, Pp. 032056, 2019.

[38] G. El-Sayed, H. Simon, and S.H. Martin, "Laser surface alloying of 316L stainless steel coated with a bioactive hydroxyapatite–titanium oxide composite", J. Mater. Sci. Mater Med., Vol. 26, Pp.83, 2015.

[39] J. Wang, Y. Chao, Q. Wan, Z. Zhu, and H. Yu., "Fluoridated hydroxyapatite coatings on titanium obtained by electrochemical deposition", Acta Biomaterialia, Vol. 5, No. 5, Pp. 1798-1807, 2009.

[40] X. Zhao, L. Yang, Yu Zuo, J. Xiong, "Hydroxyapatite Coatings on Titanium Prepared by Electrodeposition in a Modified Simulated Body Fluid", Elsevier Chinese Journal of Chemical Engineering, Vol. 17, No. 4, 2009, Pp. 667-671, 2009.

[41] H. Mas Ayua, S. Izmanb, R. Dauda, G. Krishnamurithy, A. Shah, S.H. Tomadi and M.S. Salwani, "Surface Modification on CoCrMo Alloy to Improve the Adhesion Strength of Hydroxyapatite Coating", Procedia Engineering, Vol. 184, Pp. 399 – 408, 2017.

[42] P. Rajesh, C.V. Muraleedharan, K. Manoj, and H.K. Varma, "Coating of hydroxyapatite on titanium at 200ºC by pulsed laser deposition and hydrothermal annealing, Bulletin of Materials Science, 2007.

[43] D.A. Cort, A. Menda, S. Escobedo, M.A.L opez, "Biomimetic apatite formation on a CoCrMo alloy by using wollastonite, bioactive glass or hydroxyapatite", Journal of Materials Science, Vol. 40, Pp. 3509 – 3515, 2005.

[44] F. Onderka, A. Volodarskaja, J. Kadlec, D. Dobrocký, O. Klanica, "Electrochemical Deposition of Hydroxyapatite Coatings on CoCrMo Alloy", ECS Transactions, Vol. 63, No. 1, Pp. 277-289, 2014.

[45] M.R. Shirdar, S. Izman, M.M. Taheri, M. Assadian, M.R. Abdul Kadir, "Effect of Post-Treatment Techniques on Corrosion and Wettability of Hydroxyapatite-Coated Co–Cr–Mo Alloy", Arab J. Sci. Eng., Vol. 40, Pp. 1197–1203, 2015.

[46] S. Charlena, G. Sukaryo, and M. Fajar, "Hidroxyapatite coating on CoCrMo alloy titanium nitride coated using biomimetic method", Journal of Physics: Conference Series, Vol. 776, Pp. 012056, 2016.